2011 International Conference on Computer and Software Modeling
IPCSIT vol.14 (2011) © (2011) IACSIT Press, Singapore

Theoretical Analysis and Finite Element Simulation of Behavior of Laminated Hemispherical GRP Dome Subjected to Internal Pressure

Soheil Gohari[1,a], Abolfazl Golshan[2,b] and Amran Ayob[1,c+]

[1]Faculty of Mechanical Engineering, Universiti Teknologi Malaysia, 81310, UTM Skudai, Malaysia

[2]Faculty of Mechanical Engineering, Isfahan University Technology, Isfahan, Iran

Abstract. Finite element simulation employing ABAQUS software and theoretical approaches are used to analyze the behavior of hemispherical GRP dome subjected to internal pressure. Static internal pressure and fiber angle orientation effects on meridian stress values distribution at the middle of each ply are studied. Each ply is assumed to have same thickness. Composite layup is also assumed to be symmetrical. Moreover, Language of technical computing MATLAB software is used to acquire analytical results. Meanwhile, the analytical solutions are checked through finite element simulation for validation. Static internal pressure and fiber angle orientation both are proved to linearly effect on stress distribution values in a lamination.

Keywords: Finite element simulation, Laminated hemispherical GRP dome, Static internal pressure, Fiber angle orientation, meridian and local stresses, (D/H) ratio.

1. Introduction

Composite pressurized components have vast applications in aerospace, automotive, oil and gas industries. Among these commercial products, the concept of behavior of pressure vessel components might be beneficial, particularly, in pressurized composite domes. Numerous researches have been carried out regarding failure and optimizations of composite pressure vessels. Adali and his associations found a way which laminated cylindrical pressure vessels are optimized [1]. Tauchert has some findings regarding optimum design of laminated cylindrical components [2]. J.Mistry and his associations worked on the collapse load of externally pressurized composite trospherical and hemispherical domes [3]. Roaa and his associations had some results concerning the buckling of GRP hemi-ellipsoidal dome under external hydrostatic pressure [4]. Mistry and his associations worked on the behavior of the repaired composite domes subjected to external pressure [5]. Azzam and his associations studied the comparison between analytical and experimental failure behavior of a proposed design for the filament-wound composite pressure vessels [6]. Chang obtained some results regarding experimental and theoretical analysis of first-ply failure of laminated composite pressure vessel [7]. Kam and his associations studied first-ply failure strength of laminated composite pressure vessel [8]. Cho-Chung Liang and his associations also worked on optimum design of dome contour for filament-wound composite pressure vessels based on a shape factor [9]. In most cases, the cylindrical shells are attached to dome components at the ends in which behavior of dome parts are important.

In this study, behavior of hemispherical GRP dome is investigated via both analytical and finite element simulation approaches.

[+] Corresponding author. Tel.: +60172996321,

E-mail address: soheil.gohari7@gmail.com

During the study, the thickness of each ply t is assumed to be constant and symmetric laminations are put into consideration. Comparison between the analytical and FEM simulation results employing ABAQUS and MATLAB software is used for validation and checking the accuracy of findings. Subsequently, after validation, the effect of static internal pressure and fiber angle orientations both for symmetric laminations are taken into account.

2. Theoretical Analysis

The advantage of composite material is that their alignments can be controlled. By arranging the layers and fiber angle orientations in each ply, the best arrangement can be achieved in whole layup in order to strengthen the stability of laminated composite and reduce the materials used and finally have a best design. In this study, the hemispherical GRP dome is modeled as a symmetrical laminated composite with no bending and twisting moments in each ply. Parameters as H is whole thickness layup of hemispherical GRP dome, β is fiber angle orientation named winding angle made with meridian direction, t is ply thickness which is assumed to be constant, h is the distance from the mid-ply to the ply k and D is a hemispherical dome's average diameter. The values of t and D can be obtained using Eq.1 and Eq.2, respectively. In addition, the stress resultants in the geometric coordinate axes are stated in Eq.3.

$$t = (H/k) \tag{1}$$

$$D = D_{in} + (H/2) \tag{2}$$

$$[N] = [A][\varepsilon] \tag{3}$$

Where, k is number of layers, H is total thickness, D_{in} is hemispherical dome's internal diameter, N is vector of stress resultants [N/m], A stands for extensional stiffness matrix and ε is strains vector. The relationship between stress and strains for the Kth orthotropic layer is represented in Eq.4.

$$\sigma^{(K)} = \overline{Q}^{(K)}.\varepsilon \tag{4}$$

Where $\sigma^{(K)}$ stands for vector of stresses for the Kth ply, $\overline{Q}$ is known as transformed material stiffness content (Refer to Appendix A). Local stress resultants can be obtained using Eq.5.

$$[\sigma]_K^{Local} = [T][\sigma]_K^{Global} \tag{5}$$

Where, T is transformation matrix (Refer to Appendix A) which varies as fiber angle orientation changes. Global load resultants, N_φ and N_θ, applied per unit length [N/m] in the meridian and radial directions in shell element internally pressurized (Refer to Fig. 1) can be obtained using Eq.6 and Eq.7, respectively. The shear stress value shown in Eq.8 is equal to zero due to symmetry of hemispherical dome and lamination and symmetrically loading. Moreover, dome element is thin so that the stresses and strains through thickness of the shell are negligible.

$$N_\varphi = \mathrm{Pr}\frac{r_2}{2}\left(2 - \frac{r_2}{r_1}\right) \tag{6}$$

$$N_\theta = \mathrm{Pr}\frac{r_2}{2} \tag{7}$$

$$N_{\varphi\theta} = 0 \tag{8}$$

Where, r_2 is the line between interaction of axis of revolution and the dome wall and r_1, in contrast, is meridian line representing the intersection of the dome wall and a plane containing the axis of the vessel (Refer to Fig.1). Values of r_1 and r_2 in a hemispherical dome are shown in Eq.9.

$$r_1 = r_2 = a \tag{9}$$

Where a is called inertial radius of the hemispherical dome. The effect of bending and twisting M_{φ}, M_{θ} and $M_{\varphi\theta}$ are assumed to be zero. Fig.1 and Fig.2 illustrate the dome stress resultants and the lamination geometry, respectively. After defending the dome principle equations, they must be combined with laminated composite materials theory.

The engineering constants of Graphite reinforced Polymer (Refer to Table.1) are substituted into MATLAB codes in order to obtain the output results concerning stress distribution at the middle the Kth ply. Reduced stiffness matrix and transformation matrixes both are dependent on the material properties of composite materials (Refer to appendix A). The compliance matrix, A, B and D matrixes of the composite shell internally pressurized can be shown in Eq.10, Eq.11, Eq.12 and Eq.13, respectively. By substituting the Eq.9 into the Eq.6 and Eq.7, Values of global load resultants [N/m] in hemispherical dome subjected to internal pressure can be obtained resulting in Eq.14.

$$\begin{bmatrix} N_{\varphi} \\ N_{\theta} \\ 0 \\ 0 \\ 0 \\ 0 \end{bmatrix} = \begin{bmatrix} A_{11} & A_{12} & A_{16} & B_{11} & B_{12} & B_{16} \\ A_{12} & A_{22} & A_{26} & B_{12} & B_{22} & B_{26} \\ A_{16} & A_{26} & A_{66} & B_{16} & B_{26} & B_{66} \\ B_{11} & B_{12} & B_{16} & D_{11} & D_{12} & D_{16} \\ B_{12} & B_{22} & B_{26} & D_{12} & D_{22} & D_{26} \\ B_{16} & B_{26} & B_{66} & D_{16} & D_{26} & D_{66} \end{bmatrix} \times \begin{bmatrix} \varepsilon_{\varphi} \\ \varepsilon_{\theta} \\ \varepsilon_{\varphi\theta} \\ \mathrm{K}_{\varphi} \\ \mathrm{K}_{\theta} \\ \mathrm{K}_{\varphi\theta} \end{bmatrix} \tag{10}$$

$$A_{ij} = \sum_{K\equiv 1}^{n} \left[\overline{Q}_{ij}\right]_K (h_K - h_{k-1}), i = 1,2,6; j = 1,2,6 \tag{11}$$

$$B_{ij} = \frac{1}{2}\sum_{K\equiv 1}^{n} \left[\overline{Q}_{ij}\right]_K (h_K^2 - h_{K-1}^2), i = 1,2,6; j = 1,2,6 \tag{12}$$

$$D_{ij} = \frac{1}{3}\sum_{K\equiv 1}^{n} \left[\overline{Q}_{ij}\right]_K (h_K^3 - h_{K-1}^3), \; i = 1,2,6; j = 1,2,6 \tag{13}$$

$$N_{\varphi} = N_{\theta} = \frac{P_r (a + H/2)}{2} \tag{14}$$

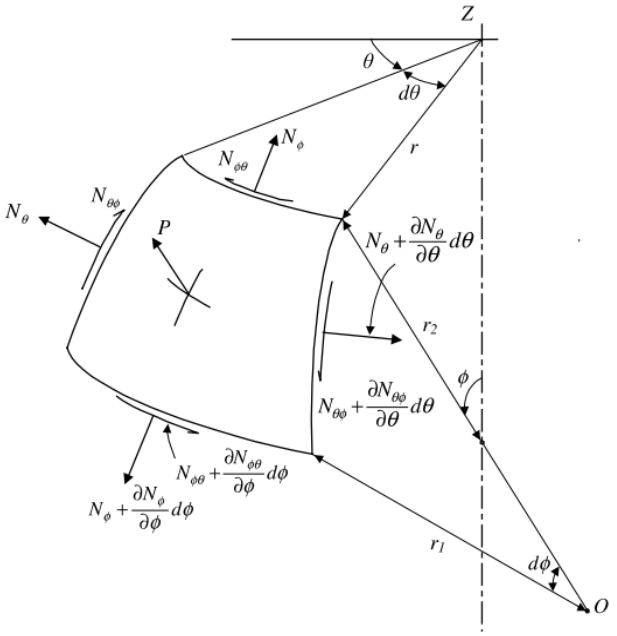

Fig.1.Direct and Shear Stress Resultant in Hemispherical Dome [9]

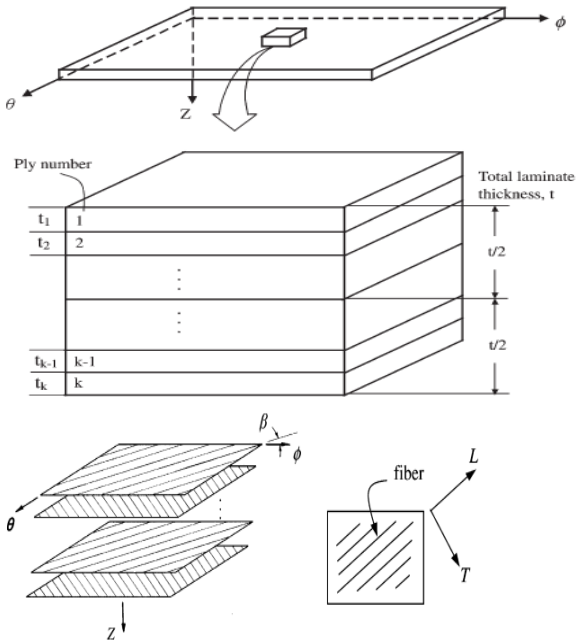

Fig.2.Schematic of a Lamination Geometry with Winding angle of Fibers [9]

3. FEM Simulation Approach

The one-layer hemispherical GRP dome subjected to value of 1[MPA] internal pressure is considered. The corresponding (D/H) ratios and meridian stress values obtained analytically are shown in Table.2. These values are acquired using Fig.6 which illustrates meridian stress behavior VS (D/H) ratios based on variety of static internal pressure applied. As assumed, k=1. Values of D can be obtained using the Eq.1 and Eq.2. Hence, for k=1 and t=0.01 [m]which are kept constant, the values of D become D= {0.38, 1.01, 0.002} [m], respectively. Therefore, based on values of D, t and k, one-layer hemispherical GRP dome must be modeled in the ABAQUS to obtain corresponding meridian stress values where winding angle with meridian axis is 0 degree ($\beta = 0$). The output result from FEM simulation must satisfy the theoretical result. The hemispherical dome is modeled with fixed boundary conditions except 1 degree of freedom in radial direction. The boundary condition is applied at the bottom of the dome. The element type selected for FEM simulation is quadratic with 8 degrees of freedom. The dome contour color spectrums before and after deformation in 1-ply hemispherical GRP dome with (D/H) =38.037 are illustrated in the Fig.4 and Fig.5, respectively. S11 represents the meridian stress values where winding angle of fibers with meridian axis are equal to zero degree ($\beta = 0$).

According to the FEM data shown in Table.3 and analytical results shown in Table.2, it is noticed that the behavior of stresses in FEM and analytical solutions are approximately same so that by increase in value of (D/H) ratio, meridian stress values rise. Schematic of comparison between FEM and analytical results for 1 [MPA] static internal pressure applied is plotted in Fig.3. The maximum error is approximately 10%.

Table.1. Material Properties of GRP (Graphite Reinforced Polymer) [GPA]

E_1	E_2	E_3	ϑ_{12}	ϑ_{21}	ϑ_{13}	ϑ_{23}	G_{12}	G_{13}	G_{23}
155	12.1	12.1	0.248	0.0194	0.248	0.458	4.4	4.4	3.2

Table.2. Analytical Solution of σ_φ in 1-Ply Hemispherical GRP Dome, Pr=1[MPA]

(D/H)=38.037	(D/H)=101	(D/H)=201
σ_φ[MPA]	σ_φ[MPA]	σ_φ[MPA]
9.509	25.25	50.25

Table.3. FEM Results of σ_φ for Arbitrarily Picked Quadratic Element with 4 Nodes and 8 Degrees of Freedom in 1-Ply Hemispherical GRP Dome, Pr=1[MPA]

(D/H)=38.037				(D/H)=101				(D/H)=201			
σ_φ[MPA]				σ_φ[MPA]				σ_φ[MPA]			
9.327	9.33	9.336	9.347	27.5	27.52	27.52	27.75	56.05	56.05	56.05	56.06

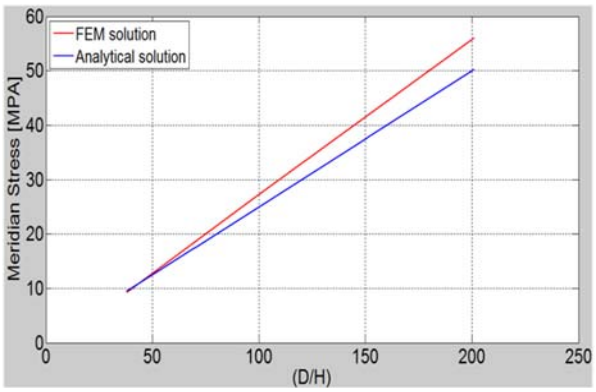

Fig.3.Comparison of the FEM and Analytical Meridian Stress Results in the Hemispherical GRP Dome at Pr=1MPA

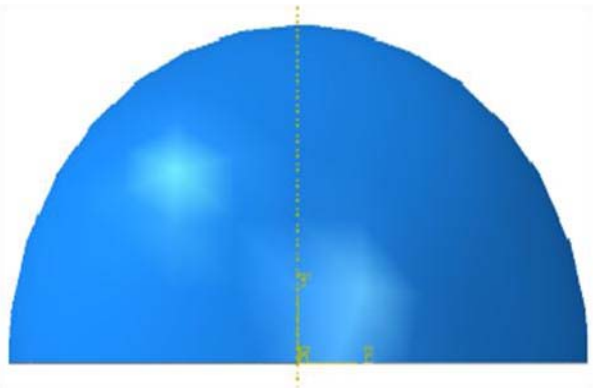

Fig.4.Front View of Hemispherical GRP dome, Pr=1[MPA], (D/H) =38.037, k=1and t=0.01[m] before Deformation

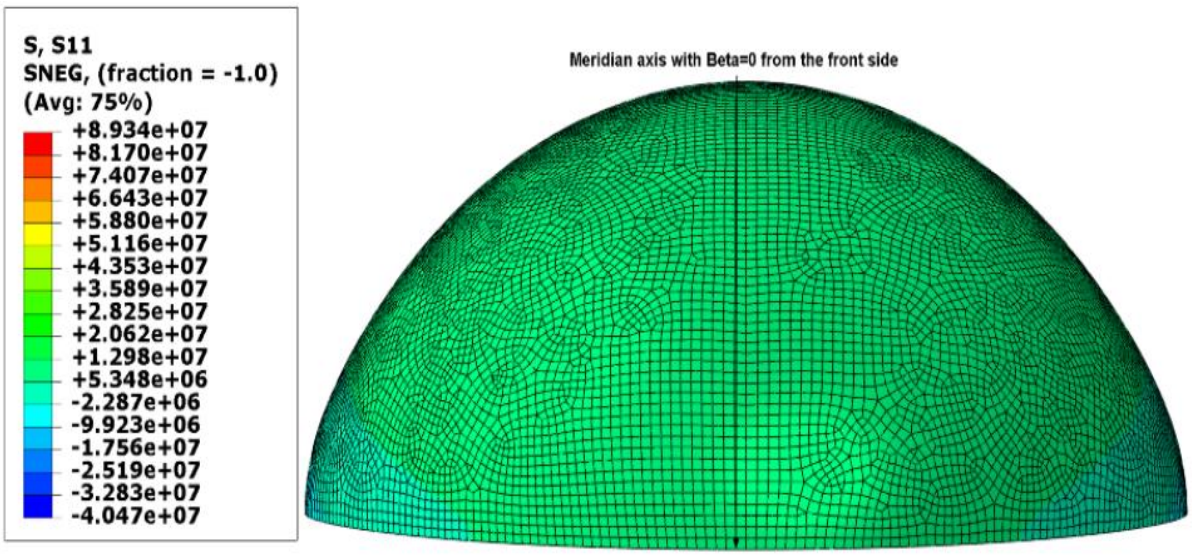

Fig.5. Front View of Hemispherical GRP Dome, Pr=1[MPA], (D/H) =38.037, k=1and t=0.01[m] after Deformation

4. Effect of Internal Pressure on Hemispherical GRP Dome Behavior

In this study, one of the purposes is to investigate the behavior of meridian stress VS (D/H) ratio, as static internal pressure varies in hemispherical GRP dome. According to Fig.6, it is noticeable that the increase in the static internal pressure makes the meridian stress values fluctuates sharply as the (D/H) ratio is kept constant. However, meridian stress varies smoothly as the (D/H) ratio rises if the static internal pressure is kept constant.

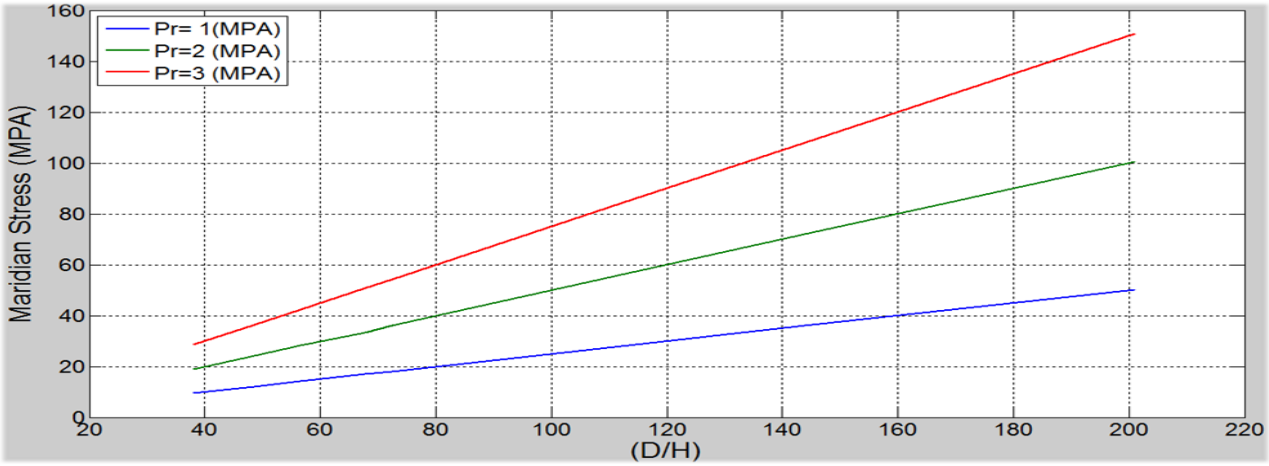

Fig.6. Effect of Internal Pressure on Meridian Stress in laminated Hemispherical GRP Dome

5. Effect of Fiber Angle Orientation on Laminated Hemispherical GRP Dome

In this step, the objective is to analyze the effect of the fiber angle orientation on local stress distributions in a laminated GRP hemispherical dome. The aim is at understanding how fiber angle orientation arrangements can effect on local stress in a lamination. The symmetrical composite laminations based on different fiber angle orientation for each ply are arbitrarily selected as below:

$$\beta_1 = \{C, C, C, C, C\}, \beta_2 = \{\pm 30, \pm 30, 0, \pm 30, \pm 30\}, \beta_3 = \{\pm 30, \pm 30, 60, \pm 30, \pm 30\},$$

$$\beta_5 = \{\pm 45 \pm, 45, 0, \pm 45, \pm 45\}, \beta_4 = \{\pm 45, \pm 45, 60, \pm 45, \pm 45\}, \beta_6 = \{\pm 60, \pm 60, 0, \pm 60, \pm 60\}$$

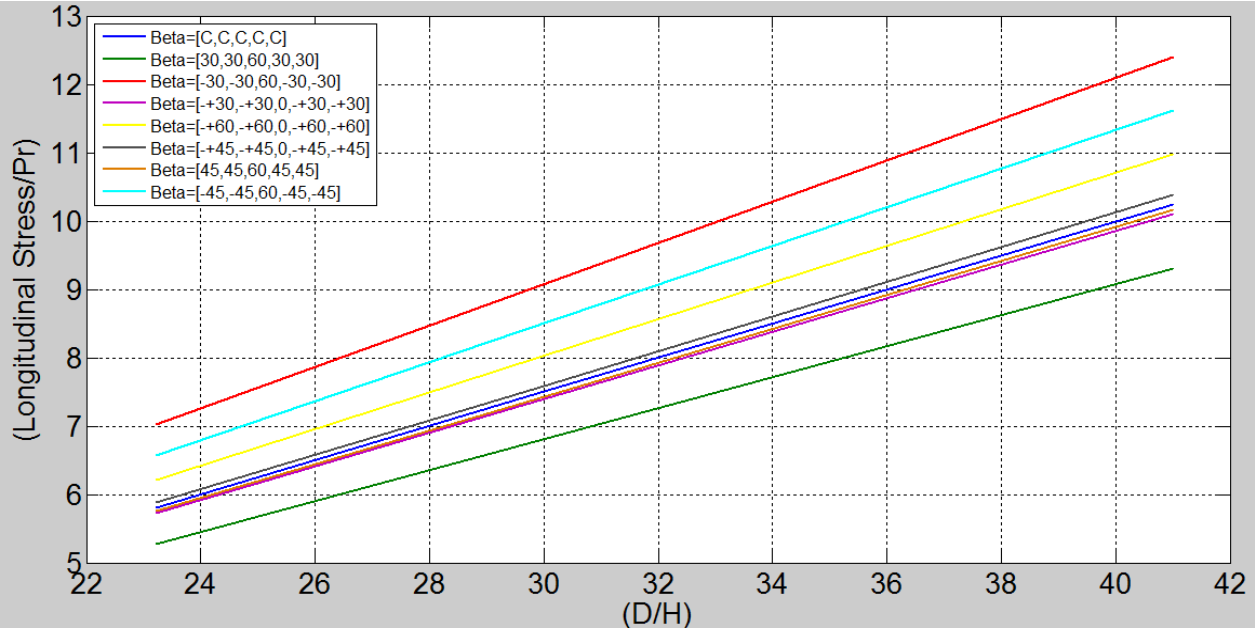

Fig.7. Effect of the Fiber Angle Orientation on the Behavior of Laminated Hemispherical GRP Dome Internally Pressurized

The Fig.7 illustrates (σ_L/P_r) VS (D/H) ratio as fiber angle orientation changes for different symmetrical laminated hemispherical GRP dome internally pressurized where longitudinal stress stands for local stress resultants along fiber orientation. According to the graphs, for same value of internal pressure, it is noticed that laminations with same winding angle $\beta = C$ kept constant for each Kth ply have same local stress values. In addition, if two laminations have fiber angle of 0 in mid-ply, winding angles with the negative and positive signs but same values have same effect on longitudinal stress behavior, however higher fiber angle orientations lead in more longitudinal stresses at middle of plies if a lamination mid-ply is not angle-ply ($\beta = 0$). According to red and dark green colors illustrated in Fig.7, it can be proved that if two laminations have the same angle-ply at the middle of lamination (for example$\beta = 60$) and same value of fiber angle orientations in other plies, the lamination with negative signs result in significantly higher longitudinal stress values at the middle of the Kth ply compared with those with positive signs. The graphs plotted also demonstrate that a non-angle ply lamination might not be chosen as a strongest layup.

6. Conclusions

As follows from foregoing analysis, after the theoretical results were validated by FEM simulation, it was observed that static internal pressure and fiber angle orientation both have the direct effect on stress distribution values (Local and global stress values both) in a laminated hemispherical GRP dome internally pressurized. Both behaviors of meridian and longitudinal stresses are linear for diverse (D/H) ratios. High (D/H) ratio results in high stress values in dome plies as static internal pressure rises. In addition, by selecting appropriate arrangement of ply's winding angles, the best and optimal layups, which basically means low stress values at each ply, can be achieved.

7. Appendix A

The elements of the reduced stiffness matrix $[\overline{Q}]$ of a laminate shown in Eq.8, Eq9 and Eq.10 are described as

$$\overline{Q}_{11} = Q_{11}c^4 + 2(Q_{12} + 2Q_{66})c^2s^2 + Q_{22}s^4 \tag{A.1}$$

$$\overline{Q}_{12} = (Q_{11} + Q_{22} - 4Q_{66})c^2s^2 + Q_{12}(c^4 + s^4) \tag{A.2}$$

$$\overline{Q}_{22} = Q_{11}s^4 + 2(Q_{12} + 2Q_{66})c^2s^2 + Q_{22}c^4 \tag{A.3}$$

$$\overline{Q}_{66} = (Q_{11} + Q_{22} - 2Q_{12})c^2s^2 + Q_{66}(c^2 - s^2)^2 \tag{A.4}$$

$$\overline{Q}_{16} = -Q_{22}cs^3 + Q_{11}c^3s - (Q_{12} + 2Q_{66})(c^2 - s^2)cs \tag{A.5}$$

$$\overline{Q}_{26} = -Q_{22}c^3s + Q_{11}cs^3 - (Q_{12} + 2Q_{66})(c^2 - s^2)cs \tag{A.6}$$

The standard transformation matrix is

$$[T] = \begin{bmatrix} c^2 & s^2 & 2cs \\ s^2 & c^2 & -2cs \\ -2cs & cs & (c^2 - s^2) \end{bmatrix} \tag{A.7}$$

Where c is $Cos(\beta)$ and s is $Sin(\beta)$

The lamina stiffness matrix $[Q]$ elements can be represented as below

$$Q_{11} = \frac{E_1}{1 - \nu_{12} \times \nu_{21}} \tag{A.8}$$

$$Q_{22} = \frac{E_2}{1 - \nu_{12} \times \nu_{21}} \tag{A.9}$$

$$Q_{12} = \frac{\nu_{12} \times E_2}{1 - \nu_{12} \times \nu_{21}} \tag{A.10}$$

$$Q_{16} = Q_{26} = 0 \tag{A.11}$$

$$Q_{66} = G_{12} \tag{A.12}$$

8. References

[1] S. Adali, E. B. Sumers, and VE. Verijenko. Optimization of laminated cylindrical pressure vessels under strength criterion. *Composite structure*; 1993, 25:305±12.

[2] T. R. Tauchert. Optimum design of a reinforced cylindrical pressure vessel. *J Comp* Mater; 1981, 15:390±402.

[3] J. Mistry, F. L. Neto, and Y. S. Wu. Collapse load of externally pressurized composite trospherical and hemispherical domes. *Advances in Engineering Software*, 1992, 15: 145-154.

[4] C. T. F. Roaa, B. H. Huat, T. B. Chei, C. M. Chong and M. D. A. Mackney. Buckling of GRP hemi-ellipsoidal dome shells under external hydrostatic pressure. *Ocean Engineering*, 2003, 30: 691-705.

[5] J. Mistry and F. L. Neto. Behavior of the repaired composite domes subjected to external pressure. *Composite*, Number 4, July, 1992, 23: 271.

[6] B. S. Azzam, M. A. A. Muhammad, M. O. A. Mokhtar, and F.A. Kolkailah. Comparison between analytical and experimental failure behavior of a proposed design for the filament-wound composite pressure vessels. *Current Advances in Mechanical Engineering Design and Production, Sixth Cairo University International MDP Conference*, Cairo, Jan: 1996: 2-4.

[7] R. R. Chang. Experimental and theoretical analysis of first-ply failure of laminated composite pressure vessel. *Journal of Composite Structure*, 2000, 49: 237-243.

[8] T. Y. Kam, Y. W. Liu, and T. Lee. First-ply failure strength of laminated composite pressure vessel. *Journal of Composite Structure*, 1997, 38: 65-70.

[9] C. C. Liang, H. W. Chen, and C-H Wang: Optimum design of dome contour for filament-wound composite pressure vessels based on a shape factor. *Journal of Composite Structures*; 2002, 58: 469-482.